ATTOSECOND DYNAMICS

Ultrafast electron dynamics in phenylalanine initiated by attosecond pulses

F. Calegari,[1] D. Ayuso,[2] A. Trabattoni,[3] L. Belshaw,[4] S. De Camillis,[4] S. Anumula,[3] F. Frassetto,[5] L. Poletto,[5] A. Palacios,[2] P. Decleva,[6] J. B. Greenwood,[4] F. Martín,[2,7]* M. Nisoli[1,3]*

In the past decade, attosecond technology has opened up the investigation of ultrafast electronic processes in atoms, simple molecules, and solids. Here, we report the application of isolated attosecond pulses to prompt ionization of the amino acid phenylalanine and the subsequent detection of ultrafast dynamics on a sub–4.5-femtosecond temporal scale, which is shorter than the vibrational response of the molecule. The ability to initiate and observe such electronic dynamics in polyatomic molecules represents a crucial step forward in attosecond science, which is progressively moving toward the investigation of more and more complex systems.

The investigation of ultrafast processes in atoms received a major stimulus with the introduction of attosecond pulses in the extreme ultraviolet (XUV) spectral region (*1*). Real-time observation of the femtosecond Auger decay in krypton was the first application of isolated attosecond pulses in 2002 (*2*). This demonstration was then followed by other important experimental results in the field of ultrafast atomic physics, such as the real-time observation of electron tunneling (*3*) and the measurement of temporal delays of the order of a few tens of attoseconds in the photoemission of electrons from different atomic orbitals of neon (*4*) and argon (*5*). The unprecedented time resolution offered by attosecond pulses has also allowed quantum mechanical electron motion and its degree of coherence to be measured in atoms by using attosecond transient absorption spectroscopy (*6*). Attosecond techniques have been applied in the field of ultrafast solid-state physics, with the measurement of delays in electron photoemission from crystalline solids (*7*) and the investigation of the ultrafast field-induced insulator-to-conductor state transition in a dielectric (*8*). In the past few years, attosecond pulses have also been used to measure ultrafast electronic processes in simple molecules (*9*). Subfemtosecond electron localization after attosecond excitation has been observed in H_2 and D_2 molecules (*10*), and control of photo-ionization of D_2 and O_2 molecules has been achieved by using attosecond pulse trains (APTs) (*11*, *12*). More recently, an APT, in combination with two near-infrared fields, was used to coherently excite and control the outcome of a simple chemical reaction in a D_2 molecule (*13*). Although the study of more complex molecules is challenging, a formative measurement of the amino acid phenylalanine has shown that ionization by a short APT leads to dynamics on a temporal scale of a few tens of femtoseconds. This has been interpreted as the possible signature of ultrafast electron transfer inside the molecule (*14*).

The application of attosecond techniques to molecules offers the possibility of investigating primary relaxation processes, which involve electronic and nuclear degrees of freedom and their coupling. In the case of large molecules (e.g., biologically relevant molecules), prompt ionization by attosecond pulses may produce ultrafast charge migration along the molecular skeleton, which can precede nuclear rearrangement. This behavior has been predicted in theoretical calculations by various authors (*15*–*19*), whose work was stimulated by pioneering experiments performed by Weinkauf, Schlag, and co-workers on fragmentation of peptide chains (*20*, *21*). This electron dynamics, evolving on an attosecond or few-femtosecond temporal scale, can determine the subsequent relaxation pathways of the molecule (*9*). The process is induced by sudden generation of an electronic wave packet, which moves across the molecular chain and induces a site-selective reactivity, which is related to charge localization in a particular site of the molecule (*15*). Although picosecond and femtosecond pulses are suitable for the investigation of nuclear dynamics, the study of electronic dynamics with these pulses has been made possible by slowing down the dynamics through the use of Rydberg electron wave packets (*22*). However, in order to study the electron wave-packet dynamics in the outer-valence molecular orbitals relevant to most chemical and biological systems, attosecond pulses are required.

Here, we present experimental evidence of ultrafast charge dynamics in the amino acid phenylalanine after prompt ionization induced by isolated attosecond pulses. A probe pulse then produced a doubly charged molecular fragment by ejection of a second electron, and charge migration manifested itself as a sub-4.5-fs oscillation in the yield of this fragment as a function of pump-probe delay. Numerical simulations of the temporal evolution of the electronic wave packet created by the attosecond pulse strongly support the interpretation of the experimental data in terms of charge migration resulting from ultrafast electron dynamics preceding nuclear rearrangement.

The α-amino acids consist of a central carbon atom (α carbon) linked to an amine (-NH_2) group, a carboxylic group (-COOH), a hydrogen

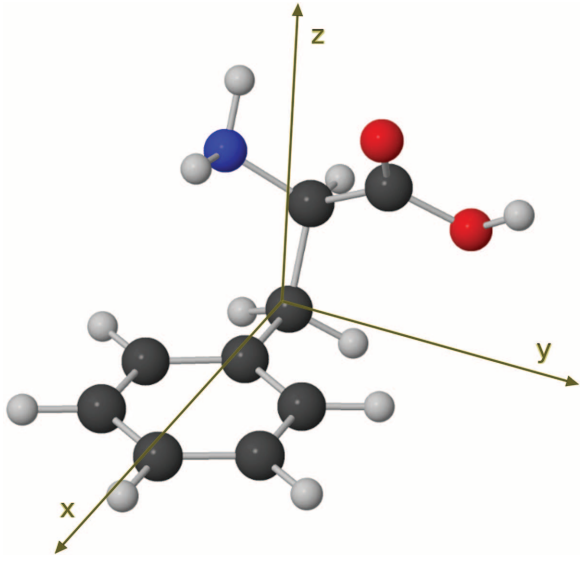

Fig. 1. Three-dimensional structure of phenylalanine. Molecular structure of the most abundant conformer of the aromatic amino acid phenylalanine. Dark gray spheres represent carbon atoms; light gray spheres, hydrogen atoms; blue sphere, nitrogen; and red spheres, oxygen. The molecular geometry has been optimized by using density functional theory (DFT) with a B3LYP functional.

[1]Institute of Photonics and Nanotechnologies (IFN)–Consiglio Nazionale delle Ricerche (CNR), Piazza Leonardo da Vinci 32, 20133 Milano, Italy. [2]Departamento de Química, Modulo 13, Universidad Autónoma de Madrid, Cantoblanco 28049 Madrid, Spain. [3]Department of Physics, Politecnico di Milano, Piazza Leonardo da Vinci 32, 20133 Milano, Italy. [4]Centre for Plasma Physics, School of Maths and Physics, Queen's University, Belfast BT7 1NN, UK. [5]IFN-CNR, Via Trasea 7, 35131 Padova, Italy. [6]Dipartimento di Scienze Chimiche e Farmaceutiche, Università di Trieste and CNR–Istituto Officina dei Materiali, 34127 Trieste, Italy. [7]Instituto Madrileño de Estudios Avanzados en Nanociencia, Cantoblanco, 28049 Madrid, Spain.
*Corresponding author. E-mail: fernando.martin@uam.es (F.M.); mauro.nisoli@polimi.it (M.N.)

atom, and a side chain (R), which in the case of phenylalanine is a benzyl group (Fig. 1). In our experiments, we used a two-color, pump-probe technique. Charge dynamics were initiated by isolated XUV sub-300-as pulses, with photon energy in the spectral range between 15 and 35 eV and probed by 4-fs, waveform-controlled visible/near infrared (VIS/NIR, central photon energy of 1.77 eV) pulses (see supplementary materials). A clean plume of isolated and neutral molecules was generated by evaporation of the amino acid from a thin metallic foil heated by a continuous wave (CW) laser. The parent and fragment ions produced by the interaction of the molecules with the pump and probe pulses were then collected by a linear time-of-flight device for mass analysis, where the metallic foil was integrated into the repeller electrode (*23*). Ionization induced by the attosecond pulse occured in a sufficiently short time interval to exclude substantial electron rearrangement during the excitation process.

We measured the yield for the production of doubly charged immonium ions as a function of the time delay between the attosecond pump pulse and the VIS/NIR probe pulse (the structure of the immonium dication is $^{++}NH_2$=CH-R). Figure 2A shows the results on a 100-fs time scale. The experimental data display a rise time of 10 ± 2 fs and an exponential decay with time constant of 25 ± 2 fs [this longer relaxation time constant is in agreement with earlier experimental results reported in (*14*)]. Figure 2B shows a 25-fs-wide zoom of the pump-probe dynamics, obtained by reducing the delay step between pump and probe pulses from 3 to 0.5 fs. An oscillation of the dication yield is clearly visible. For a better visualization, Fig. 2C shows the same yield after subtraction of an exponential fitting curve. The data have been fitted with a sinusoidal function of frequency 0.234 PHz (corresponding to an oscillation period of 4.3 fs), with lower and upper confidence bounds of 0.229 and 0.238 PHz, respectively (see supplementary materials). The experimental data have been also analyzed by using a sliding-window Fourier transform, which, at the expense of frequency resolution, shows frequency and time information on the same plot. The result is shown in Fig. 3A. At short pump-probe delays, two frequency components are present, around 0.14 and 0.3 PHz. A strong and broad peak around 0.24 PHz forms in about 15 fs and vanishes after about 35 fs, with a spectral width that slightly increases upon increasing the pump-probe delay, in agreement with the frequency values obtained from best fitting of the data reported in Fig. 2C.

From these results, we can draw the following conclusions: (i) the ultrafast oscillations in the temporal evolution of the dication yield cannot be related to nuclear dynamics, which usually come into play on a longer temporal scale, ultimately leading to charge localization in a particular molecular fragment. Indeed, standard quantum chemistry calculations in phenylalanine (see supplementary materials) show that the highest vibrational frequency is 0.11 PHz, which corresponds to a period of 9 fs, associated with X-H stretching modes, whereas skeleton vibrations are even slower, so that one can rule out that the observed beatings are due to vibrational motion. In any case, some influence of the nuclear motion cannot be completely excluded, because, for example, stretching of the order of a few picometers of carbon bonds can occur in a few femtoseconds, and this could modify the charge dynamics (*24*, *25*). (ii) Clear oscillatory evolution of the dication yield is observed even without any conformer selection. It is well known that amino acids exist in many conformations as a result of their structural flexibility. Typically, the energy barrier to interconversion between different conformers is small, of the order of a few kcal/mol, so that, even at room temperature, thermal energy is sufficient to induce conformational changes. Theoretical investigations have shown that such changes can affect the charge migration process (*26*). In the case of phenylalanine, 37 conformers have been found by ab initio calculations (*27*), with a conformational distribution that depends on temperature. In our experiment, at an average temperature of about 430 K, only the six most stable conformers are substantially present, as discussed in the supplementary materials, with the most abundant configuration shown in Fig. 1.

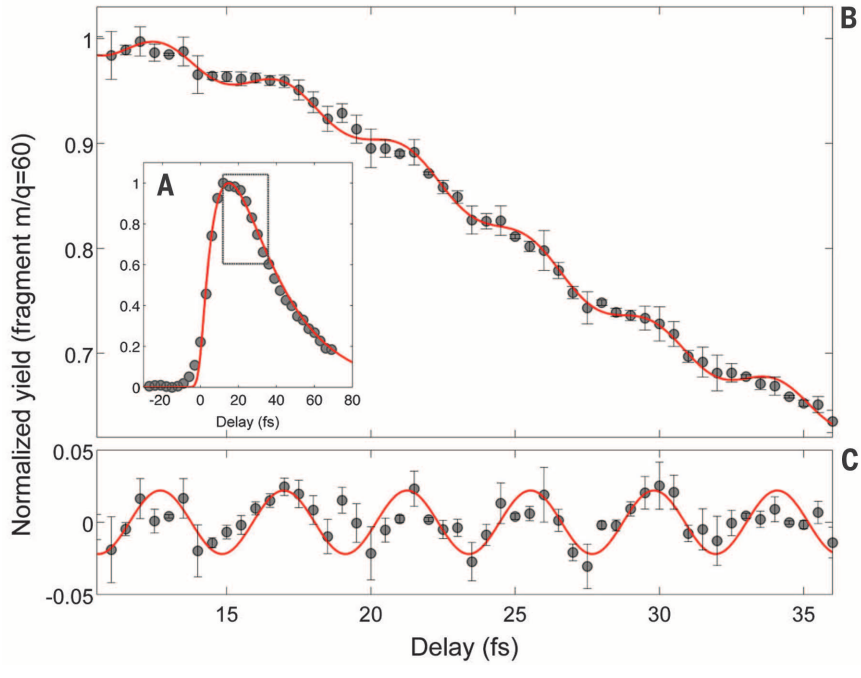

Fig. 2. Pump-probe measurements. (**A**) Yield of doubly charged immonium ion (mass/charge = 60) as a function of pump-probe delay, measured with 3-fs temporal steps. The red line is a fitting curve with an exponential rise time of 10 fs and an exponential relaxation time of 25 fs. (**B**) Yield of doubly charged immonium ion versus pump-probe delay measured with 0.5-fs temporal steps, within the temporal window shown as dotted box in (A). Error bars show the standard error of the results of four measurements. The red line is the fitting curve given by the sum of the fitting curve shown in (A) and a sinusoidal function of frequency 0.234 PHz (4.3-fs period). (**C**) Difference between the experimental data and the exponential fitting curve displayed in (A). Red curve is a sinusoidal function of frequency 0.234 PHz.

To further investigate the measured dynamics, we also varied the photon energy and spectral width of the attosecond pump pulse by inserting an indium foil in the XUV beam path. The new XUV spectrum was characterized by a 3-eV (full width at half maximum) peak centered around 15 eV, followed by a broad and weak spectral component extending up to 25 eV. In this case, doubly charged immonium fragments were barely visible, suggesting that the dication formation involves relatively highly excited states of the cation. We have calculated the energy level diagram with all the states of singly charged phenylalanine generated by the XUV pump pulse and all the states of the dication (see supplementary materials). A number of transitions from excited states of the cation to the lowest states of the dication are possible, which involve the absorption of just a few VIS/NIR photons. These states cannot be accessed by low-energy excitation, as in the case of XUV pulses transmitted by the indium foil. In this case, transitions from cation states to the lowest dication states would require the less probable absorption of many VIS/NIR photons.

We also performed theoretical calculations to describe the hole dynamics induced by an attosecond pulse similar to that used in the experiment. Details of the method can be found in the supplementary materials. Because of the high central frequency and large spectral width of the pulse, a manifold of ionization channels is open, thus leading to a superposition of many one-hole (1h) cationic states, i.e., to an electronic wave packet. Ionization amplitudes for all 1h

open channels (32 for a single conformer) were quantitatively determined by means of the static-exchange density functional theory (*28*–*30*), which has been thoroughly tested in systems of similar complexity, and first-order time-dependent perturbation theory. A calculated photoelectron spectrum at 45-eV photon energy is in very good agreement with that obtained at 100 eV in a synchrotron radiation experiment (*31*). From the ionization amplitudes, the actual electronic wave packet was calculated by using the experimental frequency spectrum of the attosecond pulse. The evolution of the electronic wave packet was then evaluated by using a standard time-dependent density matrix formalism (*6*), in which the system is described by a sum of single-particle Hamiltonians. This is a reasonable approximation when, as in the present case, changes in electronic density are mostly due to the coherent superposition of 1h cationic states induced by the XUV pulse (see supplementary materials). In other words, higher-order processes in which additional electrons are excited (e.g., correlation satellites) play a minor role in the observed dynamics. The hole-density was calculated as the difference between the electronic density of the neutral molecule, which does not depend on time, and the electronic density of the cation, from immediately after XUV excitation up to a 500-fs delay. Because, in the experiments, the molecules were not aligned, we calculated the charge dynamics resulting from excitation by pulses with the electric field polarized along three orthogonal directions (shown in Fig. 1). The results were then averaged assuming randomly oriented molecules. For a better analysis, we integrated the hole density around selected portions of the molecule: Beating frequencies were observed when the charge density was integrated around the amine group.

The six most populated conformers at 430 K were considered in the simulations. Although the precise frequencies of the relevant peaks in the calculated Fourier spectra depend on the particular conformer, the common characteristic is the presence of three dominant groups of Fourier peaks between 0.15 and 0.4 PHz. Our calculations show that the largest temporal modulation of the hole dynamics occurs around the amine group. Because of this fact, in Fig. 3C we only show the Fourier power spectrum of the calculated hole density around this group for the most abundant conformer. We have then analyzed the numerical results by using the same sliding-window Fourier transform procedure applied to the experimental data. Figure 3B shows the resulting spectrogram in a temporal window up to 45 fs, considering an experimental temporal resolution of about 3 fs. A dominant peak around 0.25 PHz is visible, which forms in about 15 fs and vanishes after about 35 fs, in close agreement with the results of the Fourier analysis of the experimental data. A higher frequency component is visible around 0.36 PHz in the delay intervals below ~15 fs and above ~30 fs. At short delays, this component favorably compares with the experimental observation of the

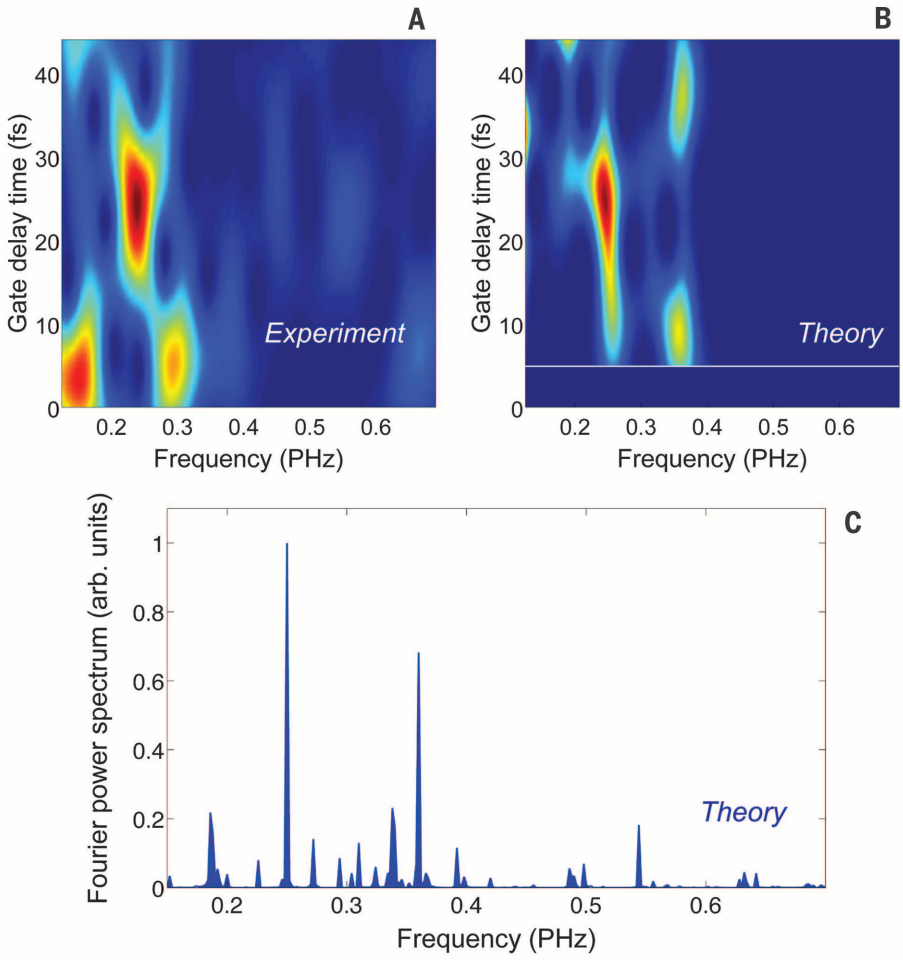

Fig. 3. Fourier analysis of charge dynamics. Spectrograms calculated for the measured data of Fig. 2C (**A**) and for the calculated hole density integrated over the amine group for the most abundant conformer (**B**). The sliding window Fourier transforms have been calculated by using a Gaussian window function $g(t - t_d) = \exp[-(t - t_d)^2/t_0^2]$, with $t_0 = 10$ fs and peak at t_d (gate delay time). The spectrogram (B) was calculated considering an experimental temporal resolution of about 3 fs. (**C**) Fourier power spectrum of the calculated hole density integrated over the amine group for the most abundant conformer.

frequency peak around 0.30 PHz in the same window of pump-probe delays. The temporal evolution of the main Fourier components is a consequence of the complex interplay among several beating processes initiated by the broadband excitation pulse. Despite the agreement with the experimental results, we cannot exclude that the nuclear dynamics, which are not included in the simulations, also play a role in the temporal evolution of the measured oscillation frequencies. The good agreement between simulations and experimental results is rather remarkable in light of the fact that simulations do not take into account the interaction of the VIS/NIR probe pulse. The fact that the effects of the probe pulse are not included in the simulations can explain why the calculated intensities of the different beatings differ from the experimental ones. We note that the beating frequencies have been observed experimentally even though the initial hole density is highly delocalized. An important result of the simulations is that the measured beating frequencies originate from charge dynamics around the amine group. This leads to the conclusion that the periodic modulations measured in the experiment are mainly related to the absorption of the probe pulse by the amine group. The mechanism that makes the probe pulse sensitive specifically to the charge density on this group is still not well understood, and therefore it will not be further discussed in the manuscript. Moreover, we observe that, in spite of the large number of potential frequency beatings associated to the wave packet motion induced by the attosecond pulse, only a few ones manifest in the experiment, thus reducing the impact of the modulations introduced by the probe pulse in the analysis of the wave packet motion. Figure 4 displays snapshots of the variation of the hole density with respect to the time-averaged hole density as a function of time for the most abundant conformer. In spite of the very delocalized nature of the hole-density resulting from the broadband XUV excitation, a

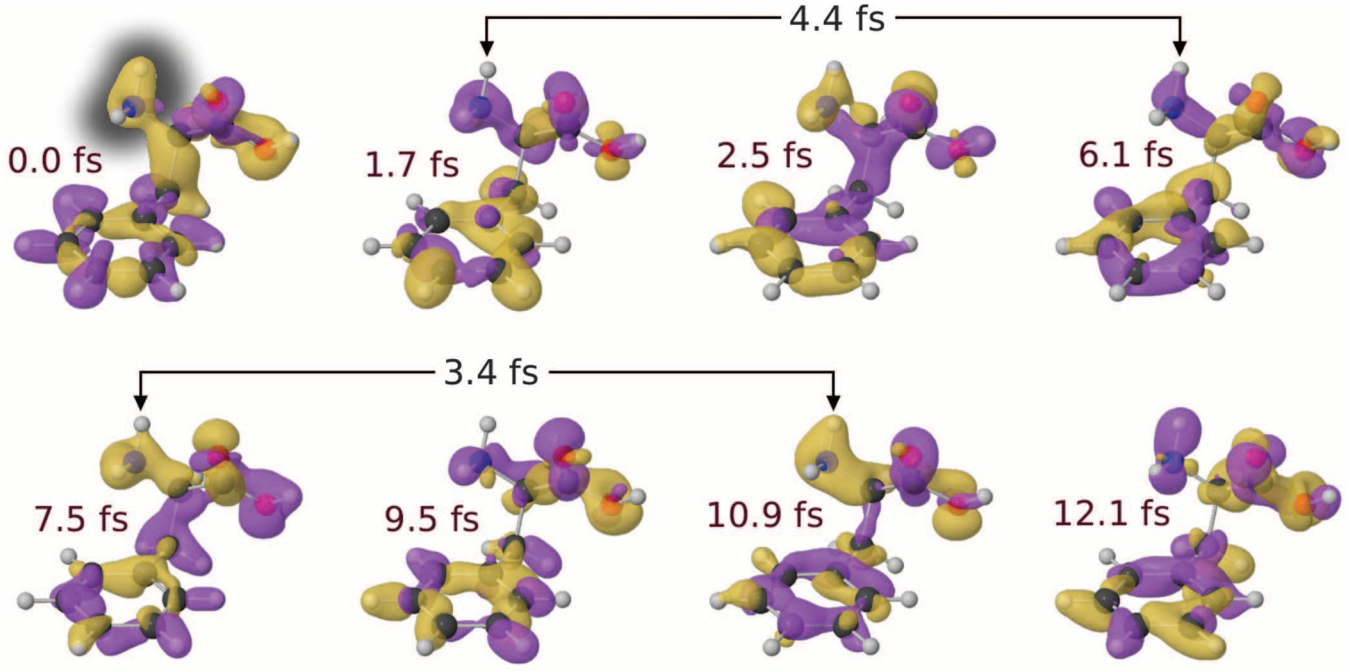

Fig. 4. Snapshots of hole dynamics. Relative variation of the hole density with respect to its time-averaged value as a function of time for the most abundant conformer. Isosurfaces of the relative hole density are shown for cutoff values of $+10^{-4}$ arbitrary units (yellow) and -10^{-4} (purple). Time is with reference to the end of the XUV pulse (first snapshot). To guide the eye, time intervals between snapshots showing a similar accumulated density over the amine group are indicated. These time intervals are close to the dominant periods associated with the electronic wave-packet motion shown in Fig. 3. The location of the amine group is highlighted in the first snapshot with a shaded contour.

substantial redistribution of this density is observed on a sub-femtosecond scale. These charge dynamics cannot be associated with a simple migration from one side of the molecule to the other. Despite the complexity of the charge configuration calculated in a realistic (i.e., experimentally accessible) situation, the concept of charge migration is still valid. In particular, the snapshots shown in Fig. 4 evidence a notable and periodic variation of the charge density around the amine group. This is because the dominant beatings always involve delocalized orbitals with substantial localization around the amine group (see supplementary materials), thus showing that evolution of the hole density around this functional group provides a highly selective interaction with the probe pulse.

Direct measurement of the ultrafast charge dynamics in an amino acid, initiated by attosecond pulses, represents a crucial benchmark for the extension of attosecond methodology to complex systems. We have demonstrated that charge fluctuations over large regions of a complex molecule such as phenylalanine can be induced by attosecond pulses on a temporal scale much shorter than the vibrational response of the system. This result was achieved in spite of the broad bandwidth of the attosecond pulses and, therefore, their low frequency selectivity, thus showing that attosecond science offers the possibility to elucidate processes ultimately leading to charge localization in complex molecules. The latter has already been achieved in hydrogen molecules, where, after attosecond excitation, charge localization was induced by the probe NIR pulse as a result of the coupling with the nuclear degrees of freedom at long time delays (*10*). A similar achievement can be envisaged in more complex molecules by performing more sophisticated experiments, e.g., as those of (*10*), combined with the extension of the existing theoretical methods to account for the nuclear motion.

REFERENCES AND NOTES

1. F. Krausz, M. Ivanov, *Rev. Mod. Phys.* **81**, 163–234 (2009).
2. M. Drescher *et al.*, *Nature* **419**, 803–807 (2002).
3. M. Uiberacker *et al.*, *Nature* **446**, 627–632 (2007).
4. M. Schultze *et al.*, *Science* **328**, 1658–1662 (2010).
5. K. Klünder *et al.*, *Phys. Rev. Lett.* **106**, 143002 (2011).
6. E. Goulielmakis *et al.*, *Nature* **466**, 739–743 (2010).
7. A. L. Cavalieri *et al.*, *Nature* **449**, 1029–1032 (2007).
8. A. Schiffrin *et al.*, *Nature* **493**, 70–74 (2013).
9. F. Lépine, M. Y. Ivanov, M. J. J. Vrakking, *Nat. Photonics* **8**, 195–204 (2014).
10. G. Sansone *et al.*, *Nature* **465**, 763–766 (2010).
11. F. Kelkensberg *et al.*, *Phys. Rev. Lett.* **107**, 043002 (2011).
12. W. Siu *et al.*, *Phys. Rev. A* **84**, 063412 (2011).
13. P. Ranitovic *et al.*, *Proc. Natl. Acad. Sci. U.S.A.* **111**, 912–917 (2014).
14. L. Belshaw *et al.*, *J. Phys. Chem. Lett.* **3**, 3751–3754 (2012).
15. F. Remacle, R. D. Levine, *Proc. Natl. Acad. Sci. U.S.A.* **103**, 6793–6798 (2006).
16. L. S. Cederbaum, J. Zobeley, *Chem. Phys. Lett.* **307**, 205–210 (1999).
17. H. Hennig, J. Breidbach, L. S. Cederbaum, *J. Phys. Chem. A* **109**, 409–414 (2005).
18. J. Breidbach, L. S. Cederbaum, *Phys. Rev. Lett.* **94**, 033901 (2005).
19. J. Breidbach, L. S. Cederbaum, *J. Chem. Phys.* **118**, 3983 (2003).
20. R. Weinkauf, P. Schanen, D. Yang, S. Soukara, E. W. Schlag, *J. Phys. Chem.* **99**, 11255–11265 (1995).
21. R. Weinkauf *et al.*, *J. Phys. Chem.* **100**, 18567–18585 (1996).
22. J. Wals *et al.*, *Phys. Rev. Lett.* **72**, 3783–3786 (1994).
23. C. R. Calvert *et al.*, *Phys. Chem. Chem. Phys.* **14**, 6289–6297 (2012).
24. S. Lünnemann, A. I. Kuleff, L. S. Cederbaum, *Chem. Phys. Lett.* **450**, 232–235 (2008).
25. D. Mendive-Tapia, M. Vacher, M. J. Bearpark, M. A. Robb, *J. Chem. Phys.* **139**, 044110 (2013).
26. A. I. Kuleff, L. S. Cederbaum, *Chem. Phys.* **338**, 320–328 (2007).
27. H. Z. Huang, W. Yu, Z. Lin, *J. Mol. Struct. THEOCHEM* **758**, 195–202 (2006).
28. D. Toffoli, M. Stener, G. Fronzoni, P. Decleva, *Chem. Phys.* **276**, 25–43 (2002).
29. E. Plésiat, P. Decleva, F. Martín, *Phys. Chem. Chem. Phys.* **14**, 10853–10871 (2012).
30. S. E. Canton *et al.*, *Proc. Natl. Acad. Sci. U.S.A.* **108**, 7302–7306 (2011).

ACKNOWLEDGMENTS

We acknowledge support from the European Research Council under ERC grant nos. 227355 ELYCHE and 290853 XCHEM, LASERLAB-EUROPE (grant agreement no. 284464, European Commission's Seventh Framework Programme), European COST Action CM1204 XLIC, the Ministerio de Ciencia e Innovación project FIS2010-15127, the ERA-Chemistry project PIM2010EEC-00751, European grants MC-ITN CORINF and MC-RG ATTOTREND 268284, UK's Science and Technology Facilities Council Laser Loan Scheme, the Engineering and Physical Sciences Research Council (grant EP/J007048/1), the Leverhulme Trust (grant RPG-2012-735), and the Northern Ireland Department of Employment and Learning.

SUPPLEMENTARY MATERIALS

www.sciencemag.org/content/346/6207/336/suppl/DC1
Materials and Methods
Supplementary Text
Figs. S1 to S11
Tables S1 and S2
References (*31*–*53*)
Movie S1

28 March 2014; accepted 16 September 2014
10.1126/science.1254061

Ultrafast electron dynamics in phenylalanine initiated by attosecond pulses

F. Calegari, D. Ayuso, A. Trabattoni, L. Belshaw, S. De Camillis, S. Anumula, F. Frassetto, L. Poletto, A. Palacios, P. Decleva, J. B. Greenwood, F. Martín and M. Nisoli (October 16, 2014)

Science **346** (6207), 336-339. [doi: 10.1126/science.1254061]

Editor's Summary

A very quick look at phenylalanine

Over the past decade, laser technology has pushed back the fastest directly observable time scale from femtoseconds (quadrillionths of a second) to attoseconds (quintillionths of a second). For the most part, attosecond studies so far have probed very simple molecules such as H_2 and O_2. Calegari *et al.* now look at a more elaborate molecule—the amino acid phenylalanine. They tracked changes in the electronic structure of the compound after absorption of an ultrafast pulse, before the onset of conventional vibrational motion.

Science, this issue p. 336

Science (print ISSN 0036-8075; online ISSN 1095-9203) is published weekly, except the last week in December, by the American Association for the Advancement of Science, 1200 New York Avenue NW, Washington, DC 20005.